AD-A122 675 SEASAT SAR SEA ICE IMAGERY FROM SUMMER MELT TO FALL FREEZE-UP(U) NAVAL OCEAN RESEARCH AND DEVELOPMENT ACTIVITY NSTL STATION MS R D KETCHUM NOV 82 1/1

UNCLASSIFIED NORDA-TN-178 F/G 8/12 NL

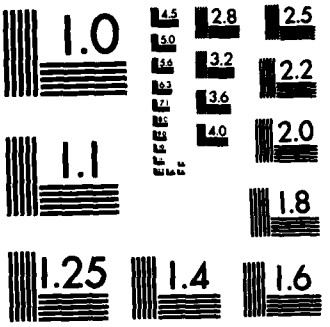

MICROCOPY RESOLUTION TEST CHART
NATIONAL BUREAU OF STANDARDS-1963-A

NORDA Technical Note 178

Naval Ocean Research and
Development Activity
NSTL Station, Mississippi 39529

SEASAT SAR Sea Ice Imagery From Summer Melt to Fall Freeze-up

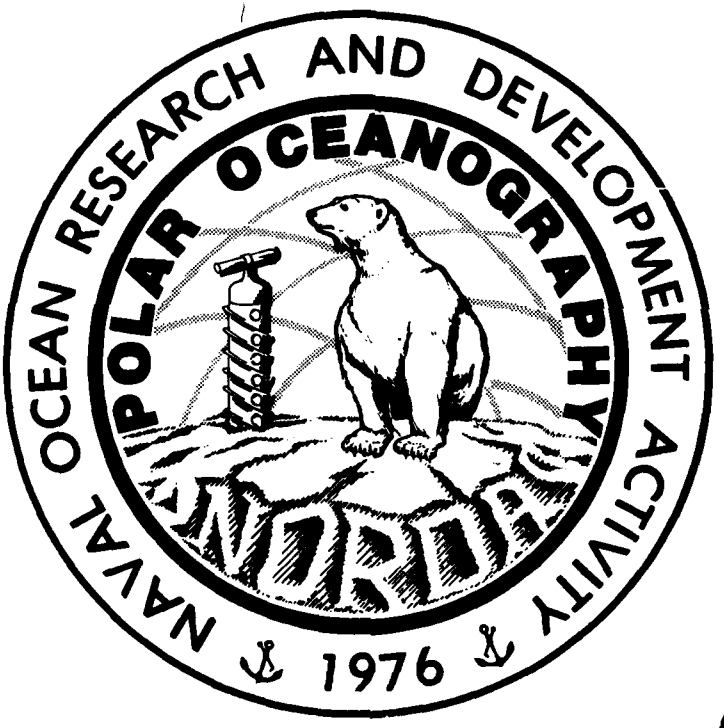

R.D. Ketchum, Jr.

Ocean Science and Technology Laboratory
Polar Oceanography Division

November 1982

ABSTRACT

Some salient aspects of SEASAT L-band SAR sea ice imagery are presented. High backscatter attributed to water-saturated surface layers reduces the ability to interpret ice conditions. Slush on water areas produces a strong backscatter which could be misinterpreted as rubble, but sequential imagery and floe sizes and shapes can be used to resolve this ambiguity. The slush effect may enhance identification of active zones. Decreasing air temperatures during fall freeze-up reduces background clutter increasing the ability to discern floe sizes and shapes. Higher SAR frequencies being considered for future satellites will show greater backscatter variations for different ice types, but many ambiguities will occur and the ability to discern ridges and floe sizes and shapes will be reduced in the marginal ice zones where interannual weather fluctuations will adversely affect surface scattering properties.

ACKNOWLEDGMENTS

This project was supported by Program Element No. 61153N, H. C. Eppert, Jr., Program Manager.

SEASAT SAR SEA ICE IMAGERY FROM SUMMER MELT TO FALL FREEZE-UP

1.0 INTRODUCTION

Naval exercises in polar seas require knowledge of the distribution of ice/water features and properties which directly or indirectly affect tactical and strategic operations. Major ice parameters of interest to submarine acoustical and tactical navigation needs are locations of ice edges, ice concentration and distribution of water openings, and ice thickness and roughness features. The last three parameters are most important to submarine functions. Cloud coverage precludes satellite observation by all except microwave remote sensors. Consequently, more emphasis is being placed on the use of microwave sensors to make synoptic observations at repeated intervals and to support operational activities on a near real-time basis. The determination of these major ice parameters can be made using airborne sensors with sufficient accuracy to satisfy most submarine operational requirements. However, the constraints on collecting airborne data such as high cost, nonavailability of aircraft, inaccessibility of some areas, and inability to cover very broad areas in a short time rule out this platform as a major practical source for the collection of synoptic data to provide forecasts or near real-time support to fleet operations. Ice edges can be estimated within limits determined by satellite passive microwave footprint size. But the ability to determine ice concentrations and the distribution of water openings, ice thickness and ice roughness from satellite passive microwave imagery is either poor or nonexistent because of the poor spatial resolution of these systems. Planned future spacecraft passive microwave systems, although improved over present systems, will not provide the information needed. In short, spacecraft synthetic aperture radar systems of the caliber of SEASAT SAR will be necessary to obtain the information needed to satisfy synoptic studies, to make reasonable forecasts, or to provide near real-time support to fleet activities. It is the only all-weather sensor capable now, or in the foreseeable future, of providing sea ice information which can be used with a high level of confidence.

The SEASAT-A synthetic aperture radar (SAR) system operated from early July 1978 to 10 October 1978. Radar sea ice imagery was collected from an 800 km altitude over large regions of the Beaufort and Chukchi Seas. Swath widths of 100 km were obtained at a resolution of 25 m. The 100 km swaths were processed as four adjacent 25 km swaths. Optical processing, performed by the Jet Propulsion Laboratory in Pasadena, California, produced 70 mm film strips having a scale of 1:500,000. Two millimeters on the 70 mm film strip represent a ground distance of one kilometer. The SAR system operated at an L-band center frequency of 1.275 GHz (23.5 cm wavelength). Horizontal polarization and a steep angle antenna mode (nominal 20.5 degrees from nadir) were employed. The technical details of the SEASAT SAR system are described by Jordon (1980).

The high resolution and broad coverage of the SEASAT SAR system allows the selection of a dense network of individual features over great distances for use in ice motion studies. These features can be reidentified on sequential imagery enabling both small scale and large scale studies. According to Hall and Rothrock (1981), SEASAT SAR imagery can provide 3-day displacements accurate to several kilometers and displacement discontinuities accurate to one or two hundred meters. High quality measurements of this sort would be ideal for studies of ice dynamics and as inputs to numerical ice prediction models.

The purpose of this paper is to look at some of the salient interpretation aspects of SEASAT SAR sea ice imagery. Unfortunately, the system failed after 99 days of operation. As a result, the satellite data obtained represent only summer conditions and transition into early fall or freeze-up. Because there were no validating underflights over the ice, correlative data are not available to aid in evaluation of the SEASAT SAR sea ice imagery. However, hypotheses are presented here to explain some variations in backscatter.

2.0 SLUSH AND WATER SATURATED ICE AND SNOW

Radical changes take place on the surface during the Arctic summer and they may occur rather rapidly. Insufficient data exist to accurately explain the interactions of summer ice and snow melt conditions with L-band radar signals, but it is evident from the SEASAT SAR imagery that the general effect is a widespread increase in radar backscatter. Based on this observation, it is hypothesized that a water-saturated surface layer of ice or snow will effectively scatter L-band signals which penetrate the layer. A widespread decrease of backscatter, seen on the SEASAT SAR imagery with the onset of freeze-up in the fall, supports this idea.

Accepting the hypothesis, it follows that areas which have a dense surface relief, and consequently, a substantial snow accumulation, have strong potential for producing a water-saturated surface layer and high backscatter during the summer season when melting processes are prevalent. Therefore, increases in backscatter during summer melt should be anticipated in rubble zones and from ridged areas of old ice and first-year ice where snow accumulation and, consequently, melt, can be high. Low relief areas of first season ice do not accumulate as much snow, hence have less melt water and should show less backscatter.

During melt conditions fresh (or very low salinity) water drains from the ice floes onto the sea water and spreads out to form a stable, very low salinity surface layer. Ice crystals will form at the interface between the fresh water layer and the underlying saline water, which may have a depressed freezing point of less than -1°C. These ice crystals will rise to the surface and the continuing process may produce a suspended layer of ice crystals. Ice crystals or slush may also result from the deposition of snow. It is hypothesized that these layers could effectively backscatter radar signals penetrating the upper water layers.

Ketchum (1981) has shown the high backscattering effects of slush on open water when using airborne L-band SAR. A similar effect was shown by Hawkins, et al.(1981) for areas which may have been either open water or frazil ice. The high backscatter produced by areas of slush-covered open water may be misinterpreted as areas of rough ice or rubble fields. This ambiguity can often be resolved with sequential imagery and coincident surface weather data. Feature sizes and shapes also provide valuable clues.

3.0 SIZE AND SHAPE ANALYSIS

A great deal of useful sea ice information can be inferred with high confidence through analysis of feature shapes and sizes by associating these parameters with dynamic events which cause them. For example, the presence of many relatively small, well-rounded, multi-year ice floes in an area strongly indicates prior intensive and extensive deformational activity, and extensively

hummocked ice can be inferred with confidence. Moreover, a low probability of undeformed first season ice types can be inferred since these types are obviously destroyed during the hummocking process. Conversely, the presence of many relatively large, and somewhat angular features suggests less intense deformational activity. In this case, undeformed first-season ice types or open water areas can be anticipated, and a smaller amount of hummocking can be inferred. These simple principles can be used as powerful tools when used to study ice dynamics by interpretation of imagery.

L-band SAR imagery is a good selection for application of these principles. At this frequency and at steep incidence angles, during the winter months, nearly all sea ice types (thicknesses) are low return targets. Floes are often delineated by high return ridges, thus enabling identification of their shapes and sizes. Accompanied by available auxiliary information, such as image sequences and coincident surface weather data, shape and size information enables reliable inference of ice conditions.

4.0 ILLUSTRATIONS AND INTERPRETATIONS

The 11 July scene (Fig. 1) in the vicinity of the northwest corner of Banks Island, Canada, shows large backscatter differences between the shorefast ice, which is primarily first-year ice, and the pack ice. The higher returns from the pack ice are attributed to water-saturated surface layers of ice or snow. First-year ice and multi-year ice, within the pack ice in this scene, are not discriminated. Apparently, the low contrast between first-year and multi-year ice and the small scale of the imagery preclude distinction of small areas of first-year ice. The high backscatter from areas between the floes is attributed to rubble and slush. Bright spots seen scattered on the floes are interpreted as slush-covered melt ponds. Much of the high backscatter seen on the shorefast ice is also attributed to slush accumulations on melt ponds and depressed water-covered areas adjacent to ridges and hummocks. The heaviest concentrations are seen along the coastline in direct association with river efflux. Transport of slush by river and land water runoff onto the shorefast ice may account for much of this accumulation. The strong backscatter from the wide offshore lead is related to the wind effects on the water surface.

Strong westerly winds associated with a low pressure system located north of the 5 August scene shown in Figure 2 pushed the pack ice against the Banks Island shorefast ice, accelerating its destruction. Evidence of recent intense deformation in the pack ice is characterized by the high backscatter hummock zones seen in close association with many lower backscatter, relatively small, rounded multi-year ice floes. During active periods in hummock zones, much slush or slush-like ice would be added to the area as a result of the tumbling and bumping action of snow-covered ice blocks. The high backscatter effect of slush, when in close conjunction with active hummocking, enhances the detection of the hummock zones. However, the above criteria are not always sufficient for an accurate interpretation because high backscatter can be caused by rubble-free, slush-covered or wind-roughened open water. For example, the high backscatter area A in Figure 2 could be mistakenly identified as a rubble zone, although the angular nature and relatively large size of the adjacent floes would argue against recent intense deformational activity in this area. The inset in the upper left corner of Figure 2 shows this area on 30 July, 6 days earlier, having much the same pattern as on 5 August, but the high returns are not present,

indicating that the high backscatter on 5 August was due either to the effects of slush or to wind on open water.

Retention of feature shape and backscatter changes, through a sequence of imagery, provide useful clues for making interpretations. In the September 8 scene in Figure 3, the broad area of high backscatter could be interpreted as wind-roughened water, slush-covered water or a rubble zone. The rounded floes in the vicinity suggest a rubble zone. The follow-up imagery of 14 and 20 September shows similar patterns of high radar return even though two low pressure systems passed over the area during this period. The changing wind speeds and directions associated with the low cell passages would have substantially changed the configuration of this area had it been only open water.

In the 14 September scene the overall radar backscatter is greater than that seen on 8 September. Many relatively small floes are contrasted against the surrounding increased backscatter. Winds were much higher on 14 September (25 knots or greater) as an intense low pressure system approached the area. The apparent increased backscatter in this scene is attributed to formation of slush-like ice and new rubble associated with hummocking related to the increased dynamic activity.

On 20 September a number of new openings are apparent in the form of dark angular shapes. These new openings probably possess a very thin new ice cover since air temperatures were 5 to 10° below freezing during the preceding four days. This significant drop in air temperatures has produced an improvement in ice surface detail by reducing background clutter. Ridged areas are now easily discriminated enabling better delineation of the ice floes.

The 25 August scene off the southwest corner of Banks Island in Figure 4 illustrates the deterioration of ice surface detail associated with advanced melt conditions. A low pressure system, which produced snowfall before this scene was imaged, had been quasi-stationary north of this area for several days. Strong northwest winds associated with the low pressure system have driven this ice southeastward from the main ice pack into open water where ice deterioration was probably accelerated. Recent breaking and disintegration of a formerly more consolidated ice field is evidenced by the irregular or jagged edges of the floes and the wide range of floe sizes. These floes are probably comprised of multi-year ice and first-year ice forms and contain ridges and hummocked zones, but distinguishing these features in this scene is difficult or impossible because of background clutter. Recent deformational activity from floe collision is evident in the highest return areas on the edges of some of the floes. High returns from the water could be in part due to a slush cover or a layer of ice crystals on the water surface. The dark or low return areas seen bordering the north and east sides of the large floes suggest a southwestward movement away from the possible slush.

With the onset of below-freezing fall temperatures, the postulated water-saturated surface layer freezes. As a result, there is a dramatic increase in surface detail and the number of identifiable features. Figure 5 shows images from the Beaufort Sea of approximately the same area of sea ice on 28 August and 18 September. On 28 August, many of the individual floes cannot be identified because background clutter obscures the bordering ridges which delineate the floes. However, on 18 September, after several consecutive days of subfreezing temperatures which reduced background clutter, numerous floes are identifiable.

The strong correlation between relatively small, rounded floes and a high degree of deformation is well illustrated in the 18 September scene. The ice backscattering characteristics shown in this image probably closely represent winter backscatter characteristics. The dark, angular features in the scene are either second-year ice (just beginning the second year's growth), new ice, or open water. The features which retained their shape over the 21 day period (marked with pointers) are identified as second year ice.

In Figure 6, additional effects of fall freeze-up are shown in the 1 October and 4 October scenes near the southwest corner of Banks Island, Canada. Northwest winds, snowfall, and air temperatures of -10°C or less prevailed during this period. The dark areas among the floes, outward from the pack ice, and along the coast in both scenes are new ice formations. The high homogeneous backscatter from the open water in the 1 October scene may be due to wind effects or ice crystal or slush formation caused by the snowfall and subfreezing air temperatures. The quick transition of much of this area to a dark new ice by 4 October supports the idea of ice crystals on the surface. In the 4 October scene the very bright band located seaward of the new shorefast ice and the many bright patches and strings among the new ice and old floes are interpreted as concentrations of slush, possibly piled up by ice motion. Strongly backscattering lines and patches of slush are also present in the new shorefast ice. It is interesting to note the different drift rates of the labeled floes in Figure 6. The smaller floes, C and D, have moved southward at a greater rate, presumably due to a quicker response to the prevailing northwest winds.

5.0 CONCLUDING REMARKS

High L-band SAR backscatter during the summer season has been attributed to a surface layer of water-saturated snow or ice and to slush and ice crystals on water surfaces. The resulting clutter effect from ice drastically reduces the ability to interpret ice conditions. A postulated high backscatter from slush-covered water could lead to misinterpretation of this type of water as hummocked zones. However, data sequences, coincident weather data, and feature sizes and shapes can be used to resolve this ambiguity. Rubble zones are indicated by the presence of many relatively small, rounded floes.

Slush formed in association with ridges and hummocks is believed to increase backscatter and enhance their detection. It is speculated that the most recent deformational activity may be identified by this phenomenon.

The imagery taken after freeze-up began is believed to closely represent that which could be taken during winter conditions--about nine months of the year. Ridges and hummock zones are clearly depicted, so that ice floe sizes and shapes are usually well delineated. Low backscatter, angular shaped areas of open water, and first season ice can be differentiated if deformational features can be detected in the first season ice. Moreover, the retention of size and shape of a low backscatter area through data sequences indicates an ice cover.

Optimum interpretations and assessments of ice conditions can be obtained by assessing the relative sizes, shapes, and backscatter of features through sequences of data along with coincident weather information. Although L-band SAR does not provide a great deal of backscatter variation for different ice types during winter conditions, it would show much more consistent backscatter than the shorter wavelengths during interannual weather fluctuations, which are

common in the marginal ice zones. L-band SAR seems to be the optimum system for delineation and portrayal of many feature shapes and sizes, criteria which are essential to the interpretation process.

X-band radar is considered by many to be an optimum frequency for ice reconnaissance. However, C-band is under consideration for future radar satellites because X-band is not considered feasible in a satellite with large area coverage requirements. Specifically, the shorter wavelength radar provides some capability to discriminate ice types using backscatter variations. The marginal ice zones are the primary areas of interest for satellite ice reconnaissance because these are key areas for commercial shipping, oil exploration and drilling, and submarine under-ice operations. Precipitation and air temperature fluctuations can be extremely variable in the marginal ice zones throughout the year. Backscatter variations seen in shorter-wavelength radar images can be strongly influenced by the effect of these variable weather conditions on the reflective properties of the ice and snow cover. This is particularly true when weather changes occur over areas of relatively thin (<1 m) first season ice which is prevalent in the marginal ice zones. Correlation of ice type (or thickness) with backscatter levels will not be as straightforward as some researchers would like to believe. Many ambiguities in interpretation should be anticipated. In addition, the presence of high-backscatter undeformed ice and snow will obscure detection of ridges and zones of hummocks.

6.0 REFERENCES

Hall, R. T. and D. A. Rothrock (1981). Sea Ice Displacement from SEASAT Synthetic Aperture Radar: J. Geophys. Res., v. 86, n. C11, p. 11, 078-082 (preprint).

Hawkins, R. K., A. L. Gray, C. E. Livingstone, and L. D. Arsenault (1981). Proceedings, Fifteenth International Symposium on Remote Sensing of Environment, Ann Arbor, Mich., May 1981, 19 p.

Jordon, R. L. (1980). The SEASAT-A Synthetic Aperture Radar System. IEEE, J. Oceanog. Eng., OE-5, p. 154-164.

Ketchum, R. D., Jr. (1981). SAR Sea Ice and Snow Signatures and Interpretation. Submitted to J. Glaciology.

Figure 1. SEASAT SAR Imagery in vicinity of NW Banks Island shows high returns related to the effects of summer melt on 11 July 1978. High returns on fast ice are largely attributed to slush on melt pools.

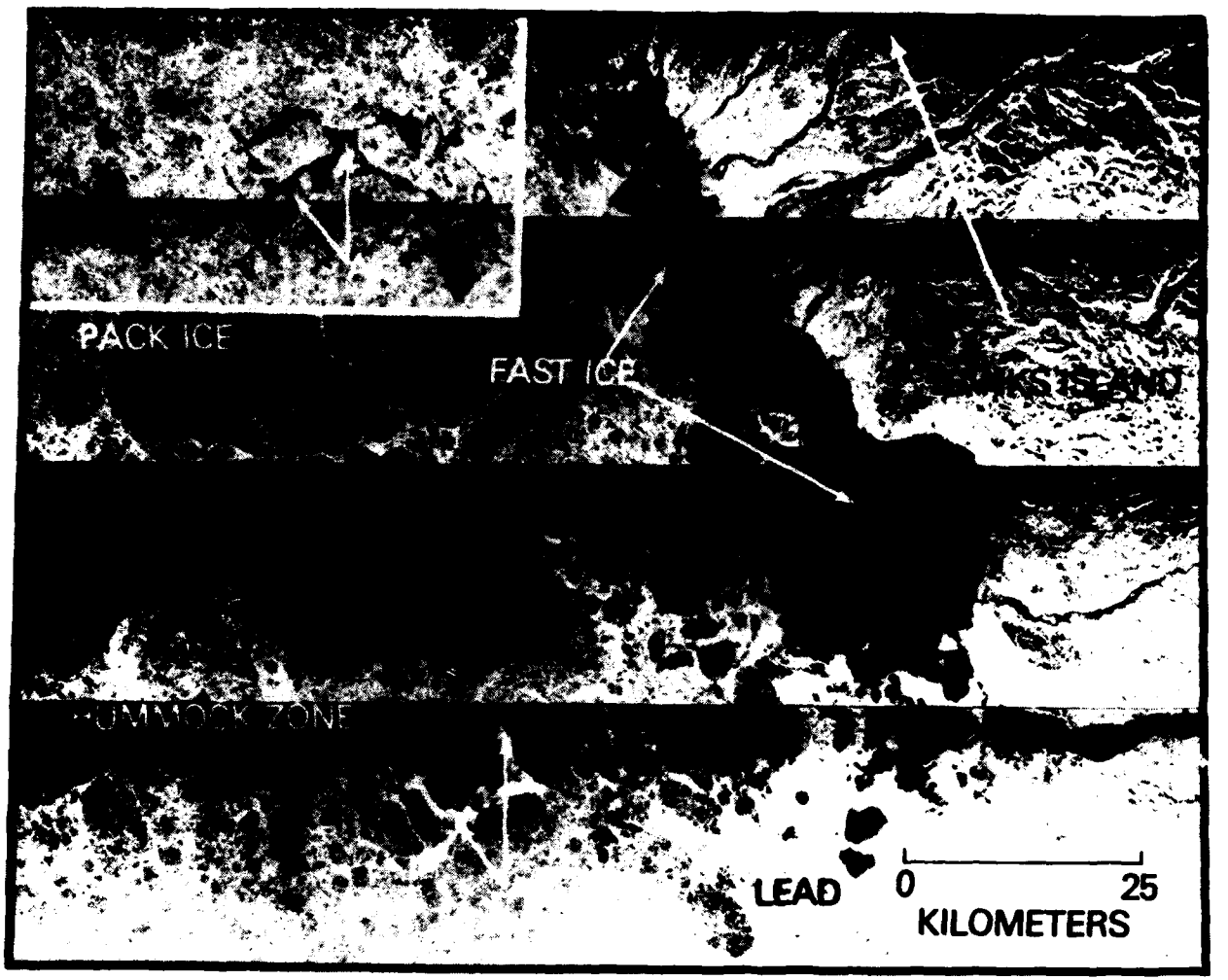

Figure 2. Beaufort Sea scene on 5 August 1978 shows high returns from hummock zones and open water areas at A. Inset shows area A on 30 July with similar pattern, but low returns indicate that the high returns on 5 August were due to wind effects or slush.

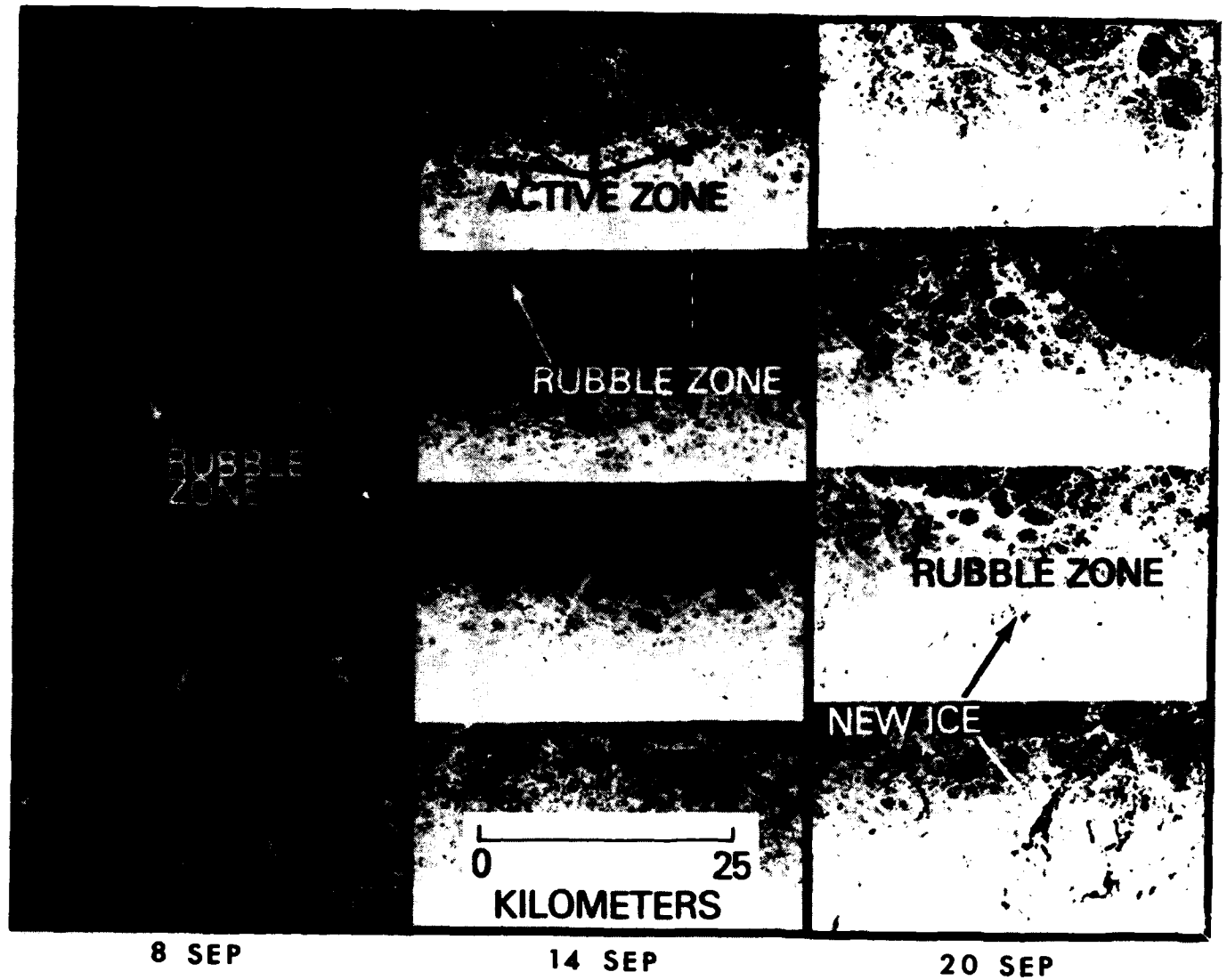

Figure 3. Retention and changes of feature shapes and backscatter through a data sequence aid interpretation. On 8 September image (left) area identified as rubble zone retains shape and backscatter characteristics. Increased backscatter on 14 September (center) identifies active zone. New low backscatter features on 20 September (right) can be identified as new ice areas.

Figure 4. Advanced melt conditions and surface deterioration are indicated by the overall high backscatter and lack of surface detail in this 25 August scene off the SW corner of Banks Island.

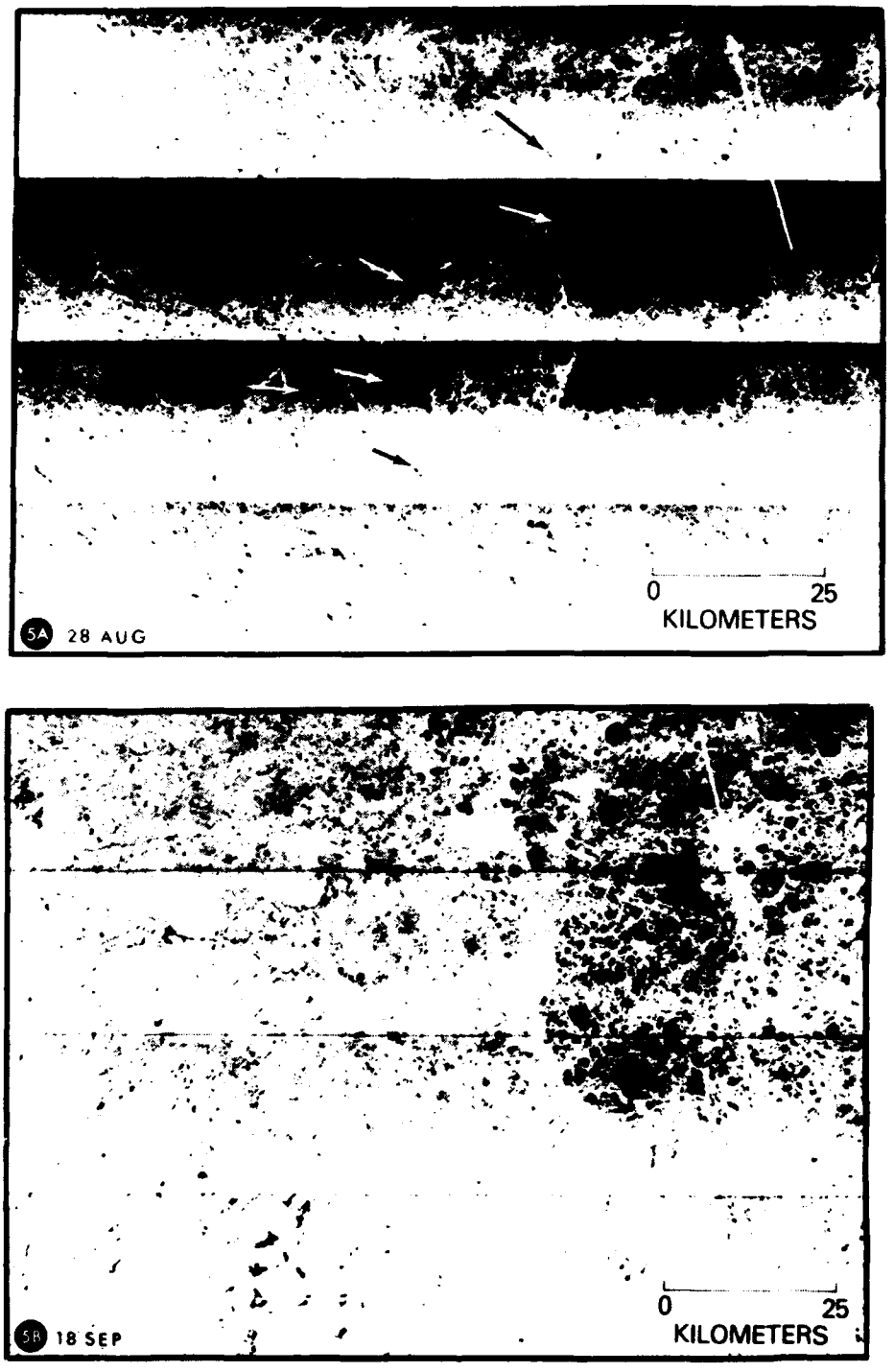

Figure 5. The effects of fall freeze-up are illustrated by the dramatic increase in detail from 28 August (upper) to 18 September (lower) in this Beaufort Sea scene.

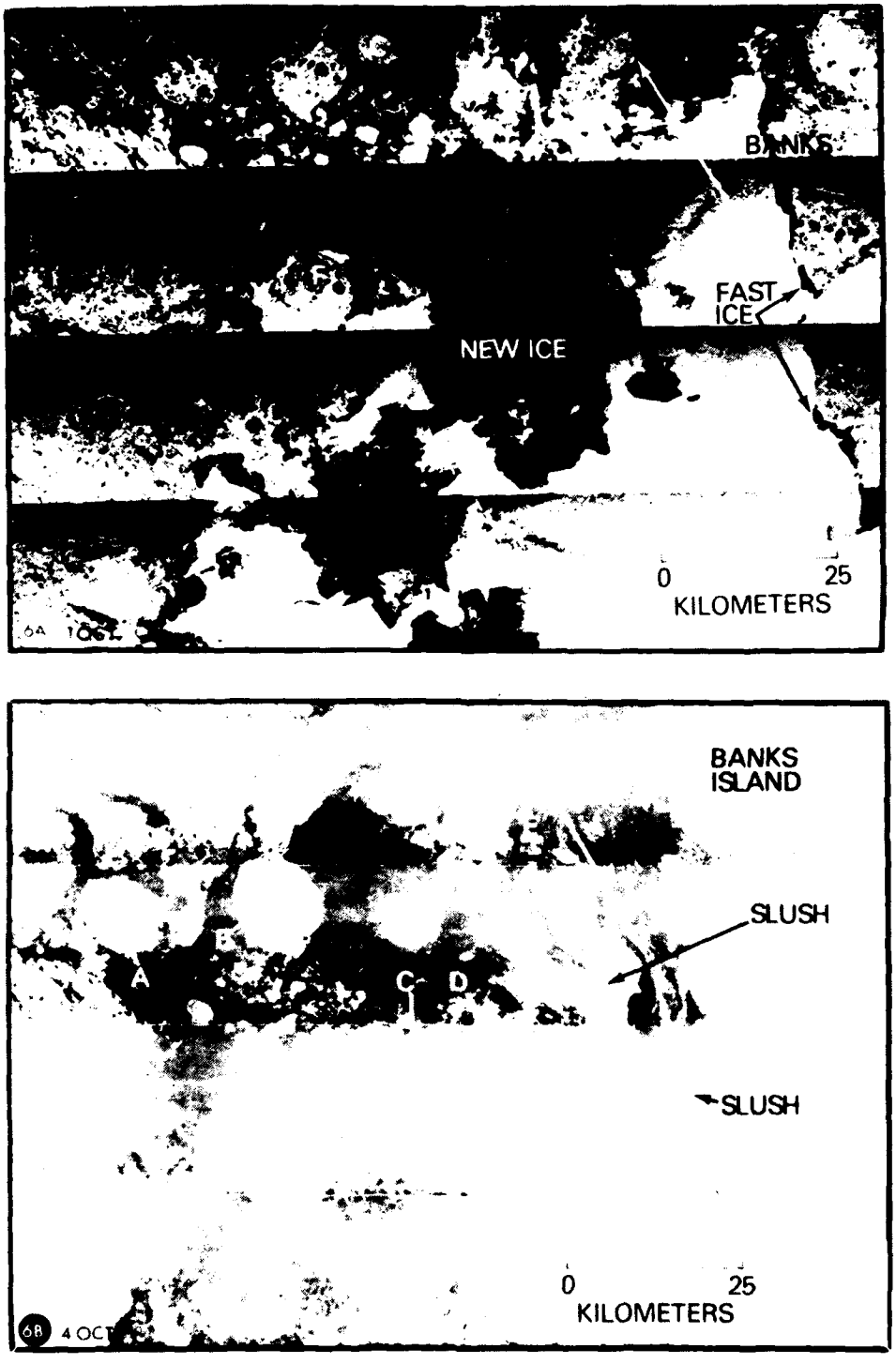

Figure 6. Dark toned new ice on open water areas is depicted off the SW corner of Banks Island on 1 October (upper) and 4 October (lower). The bright bands, patches and strings among the new ice on 4 October are believed to be concentrations of slush.

UNCLASSIFIED

SECURITY CLASSIFICATION OF THIS PAGE *(When Data Entered)*

REPORT DOCUMENTATION PAGE		READ INSTRUCTIONS BEFORE COMPLETING FORM
1. REPORT NUMBER NORDA Technical Note 178	2. GOVT ACCESSION NO. AD-A122675	3. RECIPIENT'S CATALOG NUMBER
4. TITLE *(and Subtitle)* SEASAT SAR Sea Ice Imagery from Summer Melt to Fall Freeze-up		5. TYPE OF REPORT & PERIOD COVERED Final 6. PERFORMING ORG. REPORT NUMBER
7. AUTHOR(s) R.D. Ketchum, Jr.		8. CONTRACT OR GRANT NUMBER(s)
9. PERFORMING ORGANIZATION NAME AND ADDRESS Naval Ocean Research and Development Activity NSTL Station, Mississippi 39529		10. PROGRAM ELEMENT, PROJECT, TASK AREA & WORK UNIT NUMBERS 61153N
11. CONTROLLING OFFICE NAME AND ADDRESS Naval Ocean Research and Development Activity NSTL Station, Mississippi 39529		12. REPORT DATE November 1982 13. NUMBER OF PAGES 13
14. MONITORING AGENCY NAME & ADDRESS*(if different from Controlling Office)*		15. SECURITY CLASS. *(of this report)* UNCLASSIFIED 15a. DECLASSIFICATION/DOWNGRADING SCHEDULE

16. DISTRIBUTION STATEMENT *(of this Report)*

Distribution Unlimited

17. DISTRIBUTION STATEMENT *(of the abstract entered in Block 20, if different from Report)*

18. SUPPLEMENTARY NOTES

19. KEY WORDS *(Continue on reverse side if necessary and identify by block number)*

satellite, synthetic aperture radar,
sea ice, snow, slush

20. ABSTRACT *(Continue on reverse side if necessary and identify by block number)*

Some salient aspects of SEASAT L-band SAR sea ice imagery are presented. High backscatter attributed to water-saturated surface layers reduces the ability to interpret ice conditions. Slush on water areas produces a strong backscatter which could be misinterpreted as rubble, but sequential imagery and floe sizes and shapes can be used to resolve this ambiguity. The slush effect may enhance identification of active zones. Decreasing air temperatures during fall freeze-up reduces background clutter increasing the ability to

DD FORM 1 JAN 73 1473 EDITION OF 1 NOV 65 IS OBSOLETE
S/N 0102-LF-014-6601

UNCLASSIFIED

SECURITY CLASSIFICATION OF THIS PAGE *(When Data Entered)*

(continued from Block 20)

discern floe sizes and shapes. Higher SAR frequencies being considered for future satellites will show greater backscatter variations for different ice types, but many ambiguities will occur and the ability to discern ridges and floe sizes and shapes will be reduced in the marginal ice zones where interannual weather fluctuations will adversely affect surface scattering properties.

END

FILMED

2-83

DTIC